Shroom2, a myosin-VIIa- and actin-binding protein, directly interacts with ZO-1 at tight junctions.

Raphael Etournay, Ingrid Zwaenepoel, Isabelle Perfettini, Pierre Legrain, Christine Petit, Aziz El-Amraoui

Shroom2, a myosin-VIIa- and actin-binding protein, directly interacts with ZO-1 at tight junctions

Raphaël Etournay[1,*], Ingrid Zwaenepoel[1,*,‡], Isabelle Perfettini[1], Pierre Legrain[2], Christine Petit[1] and Aziz El-Amraoui[1,§]

[1]INSERM UMRS 587, Unité de Génétique des Déficits Sensoriels, Institut Pasteur, 25 rue du Dr Roux, 75015 Paris, France
[2]Département de Biologie Joliot-Curie, CEA, 91191 Gif-sur-Yvette, France

*These authors contributed equally to this work
‡Present address: Department of Pathology and Immunology, Faculty of Medicine – CMU, 1 rue Michel Servet, CH-1211 Geneva 4, Switzerland
§Author for correspondence (e-mail: elaz@pasteur.fr)

Accepted 18 June 2007
Journal of Cell Science 120, 2838-2850 Published by The Company of Biologists 2007
doi:10.1242/jcs.002568

Summary

Defects in myosin VIIa lead to developmental anomalies of the auditory and visual sensory cells. We sought proteins interacting with the myosin VIIa tail by using the yeast two-hybrid system. Here, we report on shroom2, a submembranous PDZ domain-containing protein that is associated with the tight junctions in multiple embryonic and adult epithelia. Shroom2 directly interacts with the C-terminal MyTH4-FERM domain of myosin VIIa and with F-actin. In addition, a shroom2 fragment containing the region of interaction with F-actin was able to protect actin filaments from cytochalasin-D-induced disruption in MDCK cells. Transfection experiments in MDCK and LE (L fibroblasts that express E-cadherin) cells led us to conclude that shroom2 is targeted to the cell-cell junctions in the presence of tight junctions only. In Ca^{2+}-switch experiments on MDCK cells, ZO-1 (also known as TJP1) preceded GFP-tagged shroom2 at the differentiating tight junctions. ZO-1 directly interacts with the serine- and proline-rich region of shroom2 in vitro. Moreover, the two proteins colocalize in vivo at mature tight junctions, and could be coimmunoprecipitated from brain and cochlear extracts. We suggest that shroom2 and ZO-1 form a tight-junction-associated scaffolding complex, possibly linked to myosin VIIa, that bridges the junctional membrane to the underlying cytoskeleton, thereby contributing to the stabilization of these junctions.

Supplementary material available online at
http://jcs.biologists.org/cgi/content/full/120/16/2838/DC1

Key words: Myosin VIIa, Shroom2, F-actin, ZO-1, Tight junctions

Introduction

Epithelia have specialized intercellular structures involved in cell-cell contacts. The apical junctional complex (AJC) comprises the tight junction (TJ) and the subjacent adherens junction (AJ). The AJ is involved in initiating and maintaining adhesion between adjacent cells, whereas the TJ controls paracellular permeability and maintains cell polarity. The TJ and AJ are associated with thick bundles of actin microfilaments, which form a characteristic perijunctional actin ring at the apical pole of differentiated epithelial cells (Mooseker, 1985; Madara, 1998; Turner, 2000). Both the TJ and AJ are multiprotein complexes that consist of integral membrane proteins and the cytosolic junctional plaques (Perez-Moreno et al., 2003; Schneeberger and Lynch, 2004; Miyoshi and Takai, 2005). TJ integral membrane proteins include occludin, claudins and junctional adhesion molecules (JAMs), which interact with their counterparts at the plasma membrane of adjacent cells. Among the growing number of proteins identified in the TJ plaque is an array of PDZ-domain-containing proteins, such as members of the ZO family, which act as submembranous scaffolding molecules that bridge TJ complexes to the actin cytoskeleton. Some of these TJ proteins also participate in intracellular signaling pathways that regulate gene expression (Matter and Balda, 2003; Ivanov et al., 2005b).

Both the actin cytoskeleton and myosin II have been involved in the formation and functioning of the AJC. Active cytoskeletal rearrangements, through de novo actin polymerization, have been shown to mediate the formation of both the AJ and TJ (Vasioukhin et al., 2000; Verma et al., 2004; Ivanov et al., 2005a). This tight association to actin filaments is also responsible for the maintenance of the mature AJC (Fanning, 2001; Bershadsky, 2004). Myosin II is involved, through the Rho kinase pathway, in the localization and accumulation of E-cadherin at cell-cell contacts, thereby promoting AJ integrity (Shewan et al., 2005). Myosin II also plays a crucial role in TJ formation (Ivanov et al., 2005a). Along the same line cingulin, a peripheral component of the TJ that interacts with myosin II, has been proposed to transduce the force produced by the contraction of the actomyosin cytoskeleton to TJ proteins (Cordenonsi et al., 1999). Moreover, there is increasing evidence that the perijunctional actin ring directly regulates TJ permeability through the cortical tension generated by actomyosin contraction (Turner, 2000).

The myosin superfamily comprises myosin II (conventional myosin) and 17 classes of unconventional myosins (Krendel and Mooseker, 2005). Myosin II forms bipolar filaments that are crucial for contractile properties. By contrast, unconventional myosins do not assemble into filaments. The binding of their tails to specific proteins and/or lipids is thought

to position these motors at certain intracellular locations. The motor activity of their head is then harnessed to exert a tension on the molecules. Unconventional myosins either move along actin filaments and convey tethered vesicles and/or proteins, or anchor vesicles or proteins to actin filaments and exert a tension force on these components (Krendel and Mooseker, 2005). These motors have been implicated in a variety of cellular functions including membrane trafficking, cell movements and signal transduction (Krendel and Mooseker, 2005). Among the unconventional myosins, myosin VIIa has been proposed to be involved in cell adhesion processes. Indeed, myosin VIIa is abundant at cell-cell junctions and binds to vezatin, a putative transmembrane protein of the AJ, associated with the cadherin-catenin complex (Kussel-Andermann et al., 2000). Moreover, myosin VIIa is associated with Keap1 (a mammalian homologue of the *Drosophila* ring canal protein Kelch), a submembranous protein present in the ectoplasmic specialization, a dynamic adhesion structure that forms between Sertoli cells in the testis (Velichkova et al., 2002).

Mutations in the gene encoding myosin VIIa are responsible for the most prevalent genetic form of Usher syndrome type I (USH1), a disease characterized by congenital deafness, vestibular dysfunction, and progressive retinitis pigmentosa leading to blindness (Weil et al., 1995; El-Amraoui and Petit, 2005). With the objective of getting a deeper understanding of the role of myosin VIIa in the inner ear and retinal sensory cells, we sought proteins interacting with the tail of this myosin in the yeast two-hybrid system. We thereby identified shroom2, a protein located at the TJs of embryonic and adult epithelia.

Results

Shroom2, a submembranous PDZ-domain-containing protein, binds to myosin VIIa

The C-terminal fragment of myosin VIIa containing SH3, MyTH4 and FERM domains (aa 1605-2215; Fig. 1A) was used as the bait to screen a yeast two-hybrid mouse inner ear cDNA library (Boeda et al., 2002). Among the potential ligands isolated was a prey composed of 368 aa (aa 350-721) of the murine shroom2 (hereafter referred to as mShrm2; Fig. 1B), a member of the shroom family of proteins. The shroom family consists of four different proteins, shroom1 (Shrm1, also known as Apx) (Staub et al., 1992; Zuckerman et al., 1999), shroom2 (Shrm2, also known as Apxl), shroom3 (Shrm3, also known as KIAA1481), and shroom4 (Shrm4, also known as Kiaa1202) (Staub et al., 1992; Zuckerman et al., 1999), defined by the arrangement of at least two out of three conserved sequence motifs (Hagens et al., 2006 and references therein). By using race-PCR on a mouse vestibular cDNA library and sequence comparison with ESTs, we reconstituted a cDNA containing an entire open reading frame of 4461 bp, that displays 74% nucleotide sequence identity with the human shroom2 coding sequence. The deduced shroom2 amino acid sequence predicts a 1487 aa protein (163.5 kDa) with a PDZ domain (aa 27-107), a serine- and proline-rich domain (SPR; aa 123-326, 21% serine and 10% proline residues), the myosin-VIIa-binding region (MBR; aa 350-721), and the two Apx-Shroom domain (ASD) motifs ASD1 (aa 705-807) and ASD2 (aa 1191-1487) (see Fig. 1B).

In transfected HeLa cells expressing the GFP-tagged shroom2 MBR (GFP-mShrm2MBR) only, we observed a punctate staining throughout cell bodies and also peripheral long GFP-labeled structures associated to F-actin (open arrowheads, Fig. 1C). In co-transfected cells that express both GFP-mShrm2MBR and the myosin VIIa tail, the two proteins colocalized in the punctate structures (arrows, Fig. 1D). To further map the myosin-VIIa-binding site in shroom2, we generated a construct encoding the N-terminal part of MBR (aa 350-563), mShrm2MBRΔC. In transfected HeLa cells, GFP-tagged mShrm2MBRΔC (GFP-mShrm2MBRΔC) exhibited a diffuse cytoplasmic staining (Fig. 1E), whereas addition of the myosin VIIa tail resulted in colocalization of GFP-mShrm2MBRΔC and myosin VIIa tail (arrows, Fig. 1F). This difference in the labeling pattern suggested that this shroom2 fragment is able to interact with the myosin VIIa tail. We then tested the direct interaction between mShrm2MBR and the myosin VIIa tail by in vitro binding assays (Fig. 1G). The ^{35}S-labeled myosin VIIa tail (aa 847-2215), SH3/MyTH4/FERM (aa 1612-2215) and MyTH4/FERM (aa 1752-2215) fragments did bind to GST-mShrm2MBR, whereas a peptide containing the SH3 and MyTH4 domains only (aa 1605-1907) did not (Fig. 1G). None of the myosin VIIa fragments bound to GST alone. These results suggested that the C-terminal FERM domain of myosin VIIa mediates the interaction with shroom2. Similar experiments carried out with either the ^{35}S-labeled MyTH4 domain (aa 1752-1890) or the FERM domain (aa 1896-2215) alone, however, failed to detect any interaction with mShrm2MBR in both cases (not shown). In the reciprocal experiments, immobilized biotin-tagged myosin VIIa MyTH4/FERM or FERM fragments alone were incubated with supernatants containing GST-mShrm2MBR. The GST-tagged mShrm2MBR did bind to myosin VIIa MyTH4/FERM, but not to myosin VIIa FERM (supplementary material Fig. S1A). These results indicate that the entire C-terminal repeat, composed of both the MyTH4 and FERM domains, is necessary for the binding of myosin VIIa to shroom2. To confirm that shroom2 and myosin VIIa can form a complex in a cellular context, we carried out coimmunoprecipitation assays. Since our antibodies against myosin VIIa and shroom2 did not immunoprecipitate the corresponding proteins (supplementary material Fig. S1B-D), we used HEK293 cells expressing both Myc-tagged full-length shroom2 (Myc-mShrm2) and either the myosin VIIa tail or full-length myosin VIIa (Fig. 1H). By using the anti-Myc antibody, both the myosin VIIa tail and full-length myosin VIIa were co-immunoprecipitated with Myc-tagged shroom2 (Myc-mShrm2), but not with the Myc-tag alone (Fig. 1H). Together, these results show that shroom2 directly interacts with myosin VIIa, through the MBRΔC region and C-terminal MyTH4/FERM repeat.

Shroom2 is an F-actin-binding protein

To analyze the distribution of shroom2, we produced polyclonal antibodies against a mixture of two synthetic peptides derived from the shroom2 protein sequence (see Materials and Methods, and supplementary material Fig. S1B). Because immunofluorescence analysis of several epithelial cell lines (MDCK, LLC-PK, Caco-2 cells) showed faint shroom2 immunoreactivity (Fig. 2A), we studied the subcellular distribution of full-length shroom2 or various truncated forms in transfected cells (Fig. 2B; supplementary material Fig. S2). In MDCK cells expressing GFP-tagged full-length shroom2

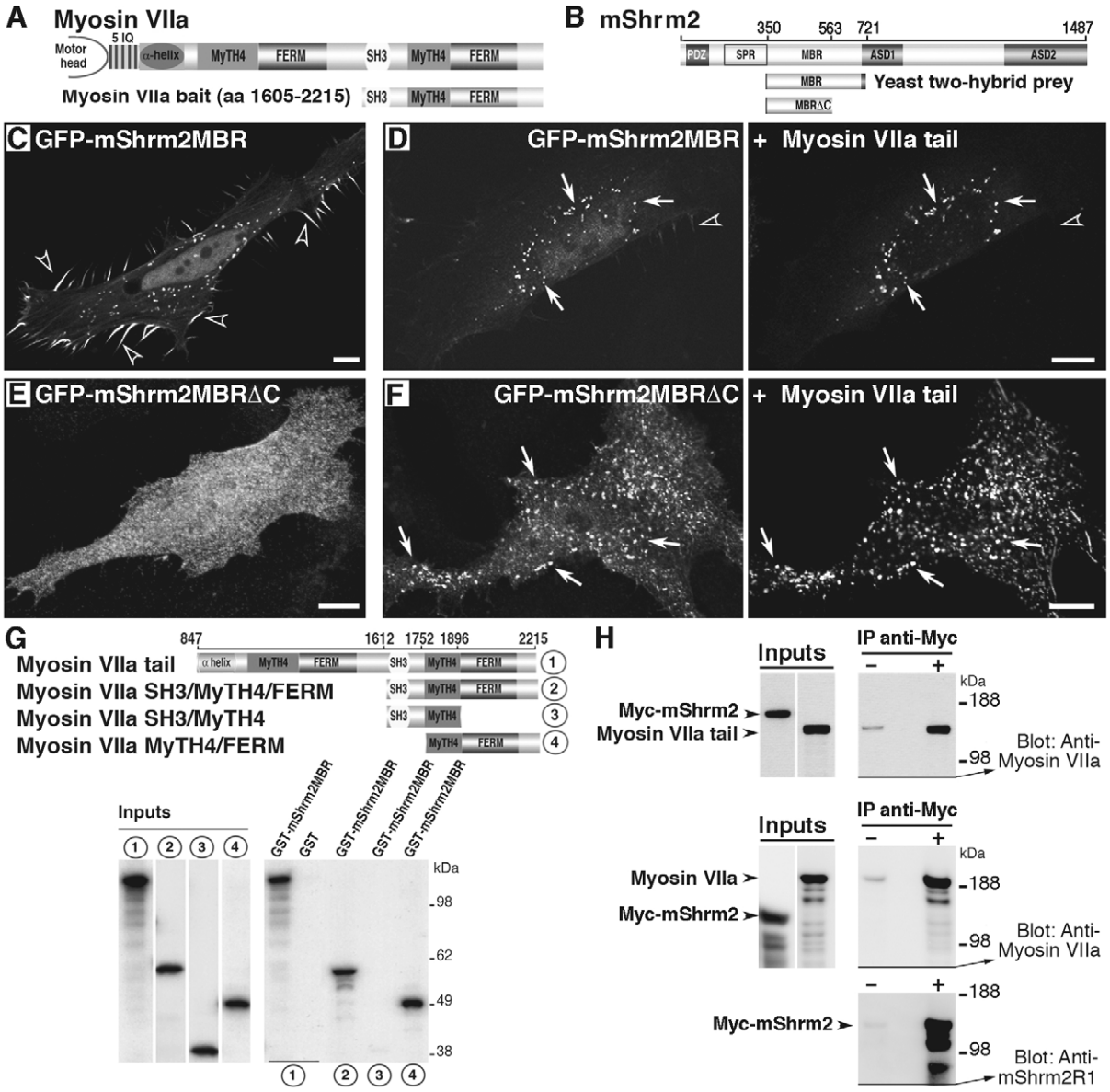

Fig. 1. Myosin VIIa binds to shroom2. (A,B) Domain structures of (A) myosin VIIa and (B) shroom2 (mShrm2). The domain composition and position of the yeast two-hybrid bait (myosin-VIIa–SH3-MyTH4-FERM) and of the prey clone (mShrm2MBR) are indicated. (B) Shroom2 consists of an N-terminal PDZ domain, an SPR, an MBR, and the ASD1 and ASD2 domains. (C) In transfected HeLa cells expressing GFP-tagged shroom2 MBR (GFP-mShrm2MBR; prey) alone, the protein exhibits a punctate cytoplasmic staining and is also particularly abundant in cytoplasmic extensions (arrowheads). (D) In co-transfected HeLa cells expressing both the prey GFP-mShrm2MBR (left panel) and Myosin VIIa tail (right panel), the two proteins colocalize in punctate structures (arrows) in the cytoplasm, arrowhead indicates cytoplasmic extension. (E) In transfected HeLa cells expressing GFP-tagged mShrm2MBRΔC (GFP-mShrm2MBRΔC, aa 350-563) alone, the fusion protein is diffusely distributed throughout the cytoplasm. (F) In co-transfected HeLa cells expressing both GFP-mShrm2MBRΔC (left panel) and Myosin VIIa tail (right panel), the two proteins colocalize in cytoplasmic punctate structures (arrows). Bars, 10 μm. (G) ^{35}S-labeled myosin VIIa fragments (1-4 in upper panel) were incubated with either GST-mShrm2MBR or GST alone (see blots in bottom panels). The ^{35}S-labeled myosin VIIa tail binds to GST-mShrm2MBR but not to GST (two lanes on left side (1) of right blot). Fragments 2 and 4 (Myosin VIIa SH3/MyTH4/FERM and Myosin VIIa MyTH4/FERM, respectively) bind to GST-mShrm2MBR (lanes 2 and 4 in right blot), whereas the SH3-MyTH4 fragment does not (lane 3 in right blot). (H) Co-immunoprecipitation assay. HEK293 cells were co-transfected with plasmids encoding either the full-length myosin VIIa and Myc-tagged shroom2 (Myc-mShrm2) or the full-length myosin VIIa and Myc tag alone (Myosin VIIa) (middle panels). The same experiment was carried out using the untagged myosin VIIa tail (Myosin VIIa tail) instead of the entire protein (top panels). Upon immunoprecipitation with the anti-Myc antibody, immunoblots were probed with antibodies against myosin VIIa or shroom2 as indicated. Both the Myosin VIIa and Myosin VIIa tail co-immunoprecipitate with Myc-mShrm2 (bottom panel).

(GFP-mShrm2), the protein was targeted to the AJC (Fig. 2B), in accordance with the endogenous shroom2 labeling. Both endogenous shroom2 and GFP-mShrm2 were more concentrated at tricellular contacts (arrowheads in Fig. 2A,B).

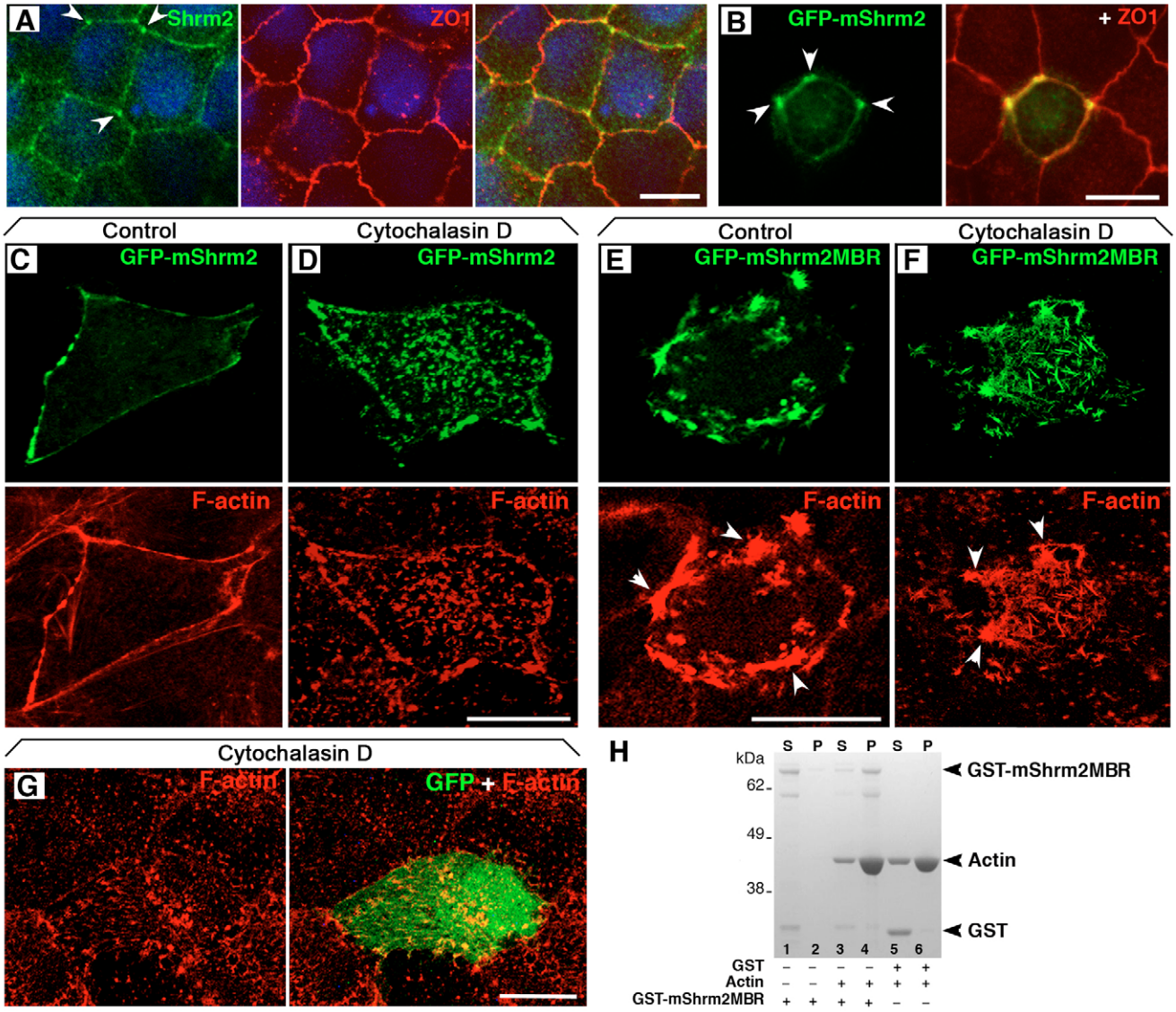

Fig. 2. Shroom2 binds to F actin. (A,B) Using (A) the anti-mShrm2R1 antibody, faint shroom2 labeling is observed in some MDCK cells, especially at cell-cell contacts. Shroom2 colocalizes with ZO-1 (yellow in right panel) especially at tricellular contacts. In (B) transfected MDCK cells that express GFP-labeled full-length shroom2 (GFP-mShrm2) a similar distribution pattern is displayed. Both endogenous shroom2 (A) and GFP-mShm2 (B) labeling is more intense at tricellular contacts (arrowheads in A and B). The TJs are visualized by ZO-1 labeling (red in A,B). (C,D) In MDCK cells expressing GFP-mShrm2 that were treated with cytochalasin D, the GFP-mShrm2 (green) colocalizes with F-actin (red), along the cell membrane. (E,F) By contrast, in cells expressing GFP-mShrm2MBR (green) that were treated with cytochalasin D, the large F-actin bundles induced by overexpression of GFP-mShrm2MBR (red) are protected against depolymerization (arrowheads). (G) In MDCK cells that express GFP alone, a diffuse GFP staining is observed in cytochalasin-D-treated cells. (H) F-actin co-sedimentation assay. Lanes 1 and 2 contain the soluble and pellet fractions of GST-mShrm2MBR, respectively, obtained upon high-speed centrifugation. GST-mShrm2MBR is not recovered in the pellet fraction (lane 2). When the same amount of GST-mShrm2MBR is incubated with F-actin at 37°C for 30 minutes (lanes 3 and 4), almost all GST-mShrm2MBR is recovered with F-actin in the pellet fraction after ultracentrifugation (lane 4). GST alone was used as a negative control (lanes 5 and 6). Bars, 20 μm.

Truncated GFP-mShrm2 fragments (GFP-mShrm2ΔPDZ, GFP-mShrm2PSP, GFP-mShrm2MBR-ASD1) were detected at cell-cell contacts, whereas GFP-mShrm2MBRΔC and a C-terminal fragment containing ASD2 gave a diffuse labeling (supplementary material Fig. S2 and data not shown). Overexpression of either GFP-mShrm2 or GFP-mShrm2MBR resulted in a significant increase of the F-actin labeling in transfected cells, compared with the non-transfected neighbouring cells (Fig. 2C,E, and supplementary material Fig. S6B). In addition, cells expressing GFP-mShrm2MBR showed many F-actin clumps (Fig. 2E). Transfected cells were treated with cytochalasin D, which binds to the barbed end of actin filaments and alters actin polymerization (Fig. 2D,F). In cells producing GFP-mShrm2, both the cortical actin filaments and the stress fibres were disrupted, and GFP-mShrm2 was detected in the same spots as F-actin (Fig. 2D). By contrast, the large filaments co-labeled for F-actin and mShrm2MBR resisted disassembly in the presence of cytochalasin D (Fig.

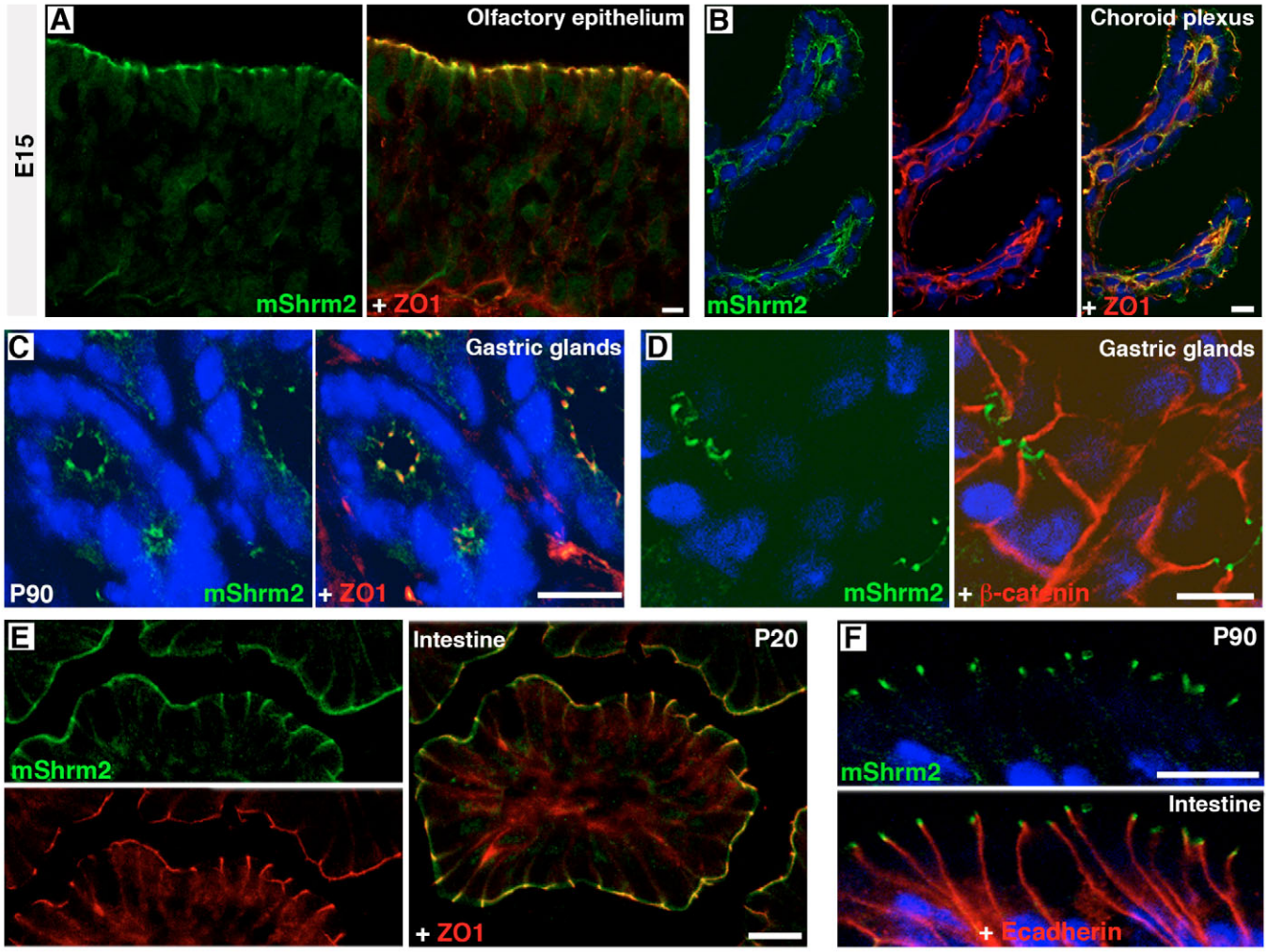

Fig. 3. Shroom2 in embryonic and adult mouse epithelia. (A,B) In embryonic mouse epithelia, at E15, the shroom2 staining (green) significantly overlaps with that of ZO-1 (red) in (A) the olfactory epithelium, and (B) the choroid plexus. (C-F) At adult stages (P20 and P90), in (C,D) the gastric glands and (E,F) small intestine, shroom2 colocalizes with ZO-1 at the TJs (yellow in C and E), but not with (D) β-catenin or (F) E-cadherin. Bars, 10 μm.

2F), thus indicating that mShrm2MBR is able to stabilize actin filaments. Dietz et al. have shown that a region of shroom2 composed partly of the MBR and the ASD1 domain (aa 513-880) binds to F-actin (Dietz et al., 2006). By in vitro co-sedimentation assays, we showed that, in the presence of F-actin, the bulk of the GST-tagged mShrm2MBR fusion protein co-sediments with F-actin, whereas in the absence of F-actin, GST-tagged mShrm2MBR is present in the supernatant (Fig. 2H). Also, MDCK cells expressing GFP-mShrm2MBRΔC (aa 350-563) exhibited a diffuse cytoplasmic labeling, with no particular colocalization with F-actin (data not shown). Together, these results suggest that the region of shroom2 that binds to F-actin, which will be referred to as ABR (for actin-binding region; aa 563-721), resides in the C-terminal part of MBR (see supplementary material Fig. S7A).

Shroom2, a TJ protein of embryonic and adult epithelia

To explore the relevance of shroom2 association with the actin cytoskeleton, we analyzed subcellular distribution of shroom2 in vivo. In agreement with the results obtained by Dietz et al. (Dietz et al., 2006), shroom2 was detected at the AJC of mouse embryonic epithelial and endothelial cells (Figs 3, 4, 5). We further explored shroom2 distribution in adult mouse epithelia. Shroom2 labeling was detected at the most apical border of cell-cell contacts in all tested epithelia, i.e. in the nasal cavity, brain, inner ear, retina, submandibular gland, lung, liver, pancreas, stomach, intestine, kidney and testis (Figs 3, 4, 5, supplementary material Fig. S3, and data not shown). Expression of mShrm2 in neuronal processes may be associated with the TJ-like structures that form between the myelin sheath lamellae (Dermietzel and Kroczek, 1980). Because some of the retinal and inner ear anomalies in myosin-VIIa-defective mice (Liu et al., 1998; Self et al., 1998; Liu et al., 1999) might result from a disruption of the interaction between myosin VIIa and shroom2, we focused on the distribution of shroom2 in these sensory organs. In the retina, shroom2 was first detected at embryonic day 12 (E12) in the differentiating pigment epithelium, and the labeling then increased from E14 onwards (Fig. 4A-C). Analysis at 3 weeks and at 3 months of age showed that the bulk of shroom2

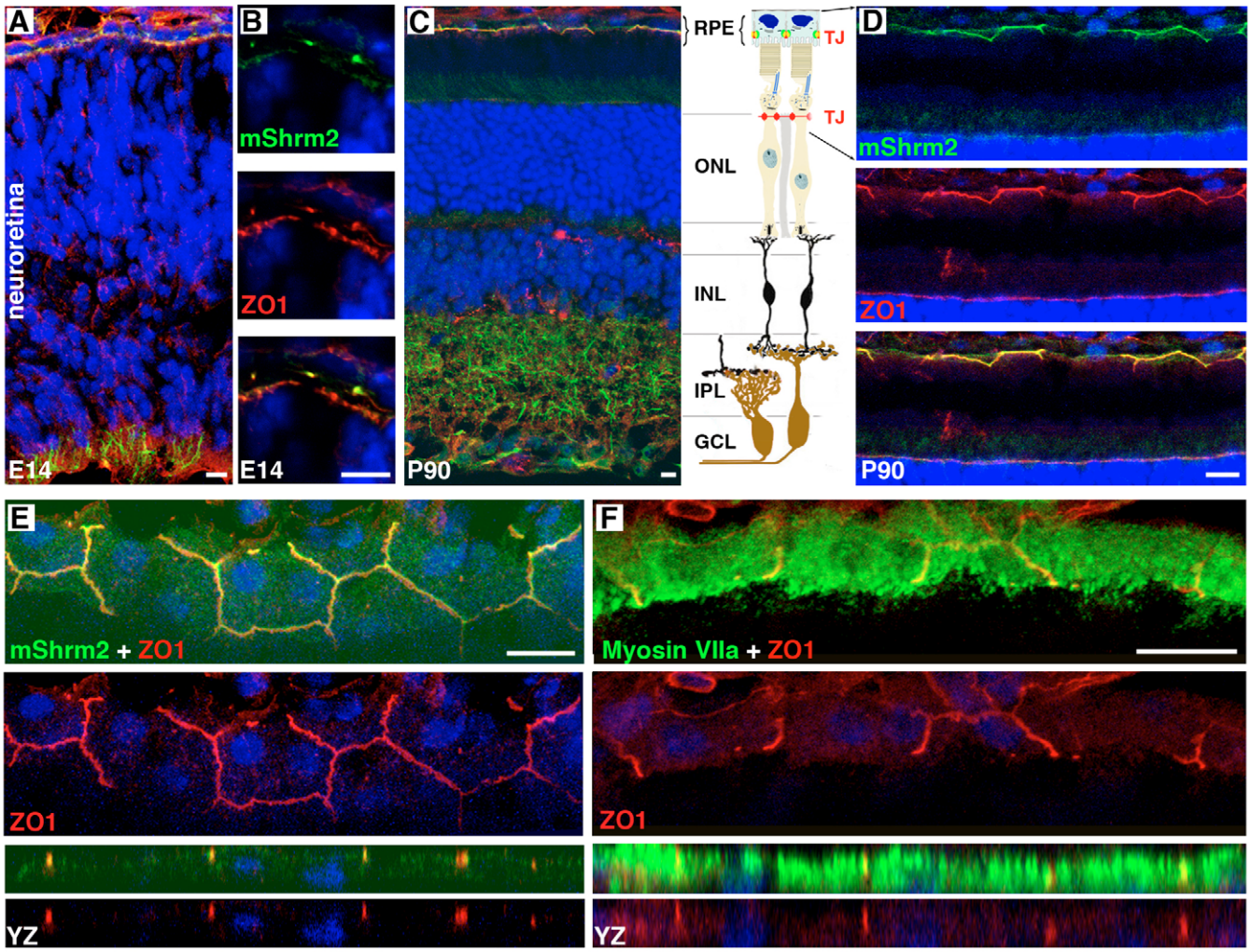

Fig. 4. Shroom2, myosin VIIa and ZO-1 in the mouse retina. (A-F) Sections of the mouse retina at (A,B) E14 and P90 (C-F). Shroom2 is detected in the retinal pigment epithelium (RPE) cells, and some neuronal extensions in the inner region of the neuroretina. (C-F) Shroom2 is concentrated at the TJs, where it is co-distributed with ZO-1 (red). The neuronal labeling of shroom2 persists in adults, in the inner plexiform layer (IPL). (E,F) Adjacent tangential sections of the P90 mouse retina labeled for ZO-1 and either shroom2 or myosin VIIa. Note that shroom2 is co-distributed essentially with ZO-1 at the TJ zone, whereas myosin VIIa is present throughout the cytoplasm, and in the apical microvilli. Colocalization with ZO-1 is illustrated in the confocal orthogonal (*YZ*) reconstructions. ONL, outer nuclear layer; INL, inner nuclear layer, GCL, ganglion cell layer. Bars, 10 μm.

immunoreactivity is in retinal pigment epithelium (RPE) cells (Fig. 4C,D, supplementary material Fig. S4), and also in some neuronal extensions in the inner plexiform layer of the neuroretina, where bipolar cells and interneurons of the inner nuclear layer synapse with ganglion cells (Fig. 4C). In the inner ear, the shroom2 labeling progresses differently during the morphogenesis period and maturation steps of the auditory organ (Fig. 5). Intense staining of shroom2 showed that it was equally distributed at the apical part of all epithelial cells facing the luminal space of the early developing cochlear and vestibular organs (Fig. 5A and data not shown). At late embryonic and postnatal stages in the cochlea, strong shroom2 labeling was detected at the tightly joined apical surfaces of sensory cells (hair cells) and supporting cells, that form the reticular lamina (Fig. 5B-D; supplementary material Fig. S5B), and in the apical region of the stria vascularis marginal cells (Fig. 5E, supplementary material Fig. S5A). Notably, the labeling was even more intense at tricellular contacts (arrowheads in Fig. 5E). Labeling of Shroom2 and myosin VIIa overlapped in the apical region of cochlear (Fig. 5F; supplementary material Fig. S5B) and vestibular (not shown) hair cells. Analysis of shroom2 in the hair cells of myosin VIIa defective *shaker-1*^{B4626SB} mice, did not show any significant alteration in the distribution of shroom2 (Fig. 5G), suggesting that myosin VIIa is not required for targeting of shroom2 to the TJ in hair cells.

Double immuno-labeling experiments with TJ and AJ markers were carried out in various epithelia to define the precise shroom2 distribution within the AJC. In all the analyzed epithelia, i.e. olfactory epithelium (Fig. 3A), choroid plexus (Fig. 3B), gastric glands (Fig. 3C,D), intestinal cells (Fig. 3E,F), retinal pigment epithelial cells (Fig. 4D, supplementary material Fig. S4) and inner ear epithelial cells (Fig. 5A-D, supplementary material Fig. S5B), we found that

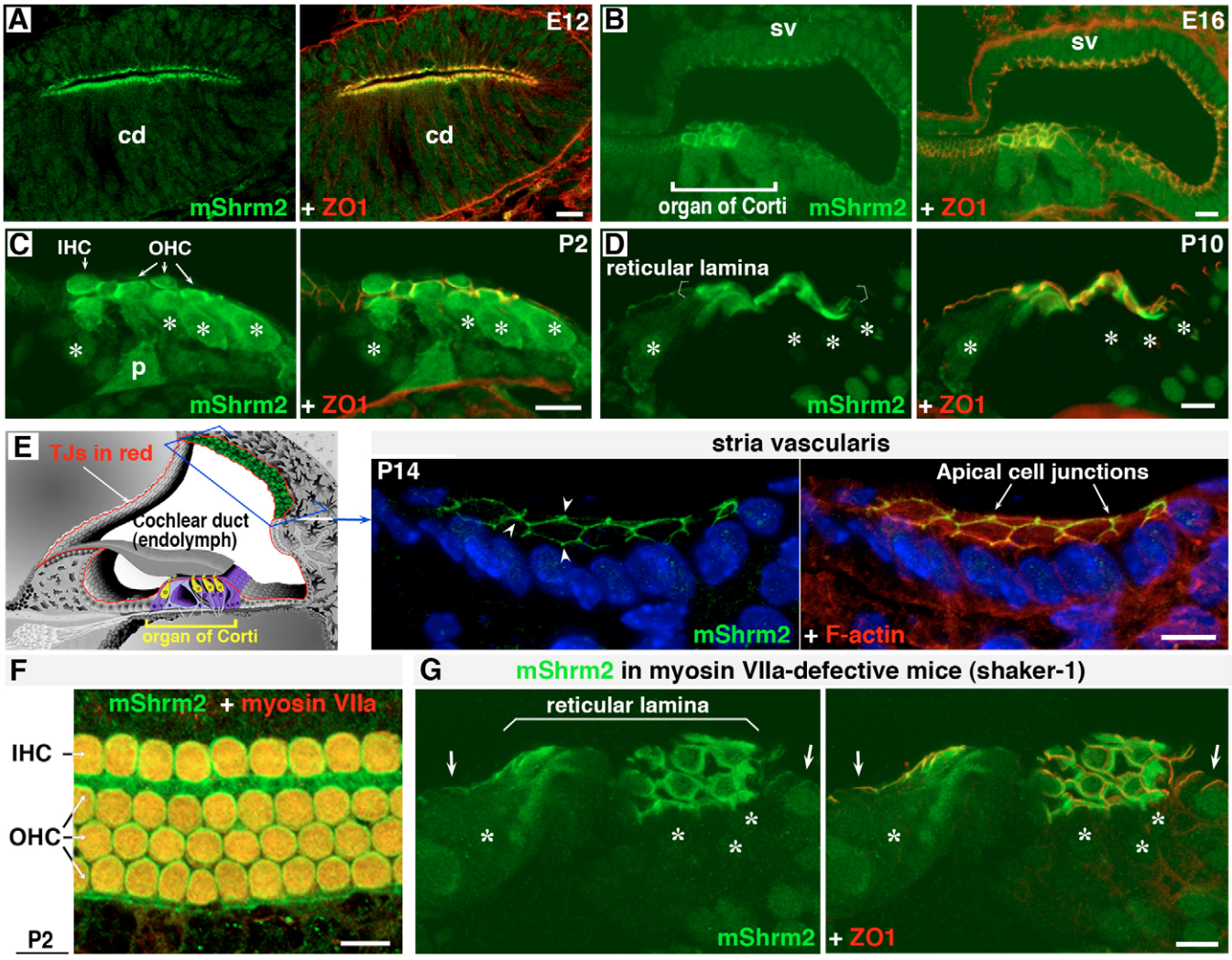

Fig. 5. Spatiotemporal shroom2 distribution in the mouse auditory epithelia. (A-D) At E12, shroom2 colocalizes with ZO-1 at the apical surface of all the epithelial cells delineating the cochlear duct (cd) (A). As development proceeds, the shroom2 labeling becomes more intense in the sensory epithelium (organ of Corti) (B). At birth, a transient diffuse labeling is observed throughout the cytoplasm of the sensory inner (IHC), and outer (OHC) hair cells (* over cell bodies), and pillar (p) cells (C). This cell body labeling decreases at later stages, and is not detected from P10 onwards (D). The bulk of shroom2 labeling is associated with the tightly joined apical domains of the hair cells and their adjacent supporting cells, forming the reticular lamina (D), and also at the apical cell-cell junctions of the marginal cells in the stria vascularis (arrowheads in E). The stria vascularis is a bilayer epithelium of the cochlear duct lateral wall, which secretes K^+ in the endolymph (the fluid filing the cochlear duct) and produces the endocochlear potential. (F) Whole-mount preparation of a mouse organ of Corti at P2, illustrating the codistribution of shroom2 and myosin VIIa. (G) The absence of myosin VIIa in shaker-1 mutant mice does not alter the normal targeting of shroom2 in the hair cells. Stronger shroom2 labeling is observed in the reticular lamina, whereas weaker labeling is seen in other supporting cells (arrows). Bars, 10 μm.

shroom2 colocalized with occludin (not shown), and ZO-1 (also known as TJP1) at the apical most border. By contrast, no significant colocalization was observed between shroom2 and the AJ proteins β-catenin and E-cadherin (Fig. 3D,F; and supplementary material Fig. S3D). We conclude that shroom2 is preferentially targeted to the TJs, in embryonic and adult epithelia.

Shroom2 targeting requires pre-existing TJs

To get insight of the role shroom2 plays in the formation and/or the maintenance of TJs, we studied the distribution of GFP-mShrm2 during the establishment of cell-cell contacts in MDCK cells. The cells were analyzed at various times during the formation of contacts between cells. In isolated and non-confluent cells, GFP-mShrm2 displayed a cytoplasmic staining and colocalized with F-actin (Fig. 6A). In islands of differentiating MDCK cells, we observed shroom2 associated with the plasma membrane exclusively at the sites of initial cell-cell contacts (arrowheads Fig. 6B). However, shroom2 was not recruited to all cell-cell contacts, visualized by the ZO-1 staining (arrows, Fig. 6B; and supplementary material Fig. S6A). As cells became confluent and cell-cell junctions more differentiated, both GFP-mShrm2 and ZO-1 were broadly distributed along the junctional sites (Fig. 6C, and

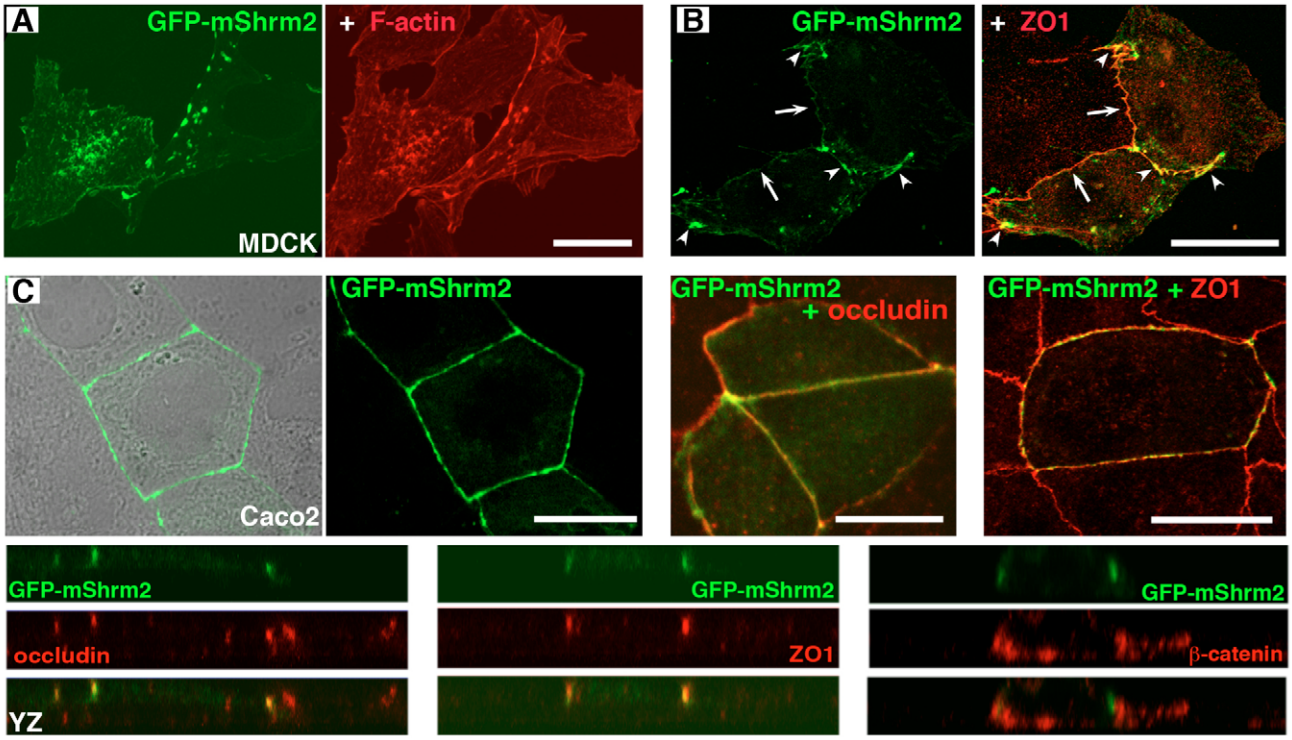

Fig. 6. Shroom2 targeting requires the presence of TJs. (A) In non-confluent MDCK cells, GFP-mShrm2 displays a punctate labeling, that perfectly colocalizes with F-actin (red) in the cytoplasm or beneath the plasma membrane. (B) In nascent cell-cell contacts, as shown in the peripheral cells of MDCK islands, GFP-mShrm2 is recruited to the plasma membrane at the AJC. GFP-mShrm2 is present in some (arrowheads) but not all junctional regions visualized by ZO-1 labeling (arrows). (C) Upon cell confluency, GFP-mShrm2 spreads to all junctional sites, as shown in Caco-2 cells. In these cells, GFP-tagged shroom2 colocalizes with occludin and ZO-1 but not with β-catenin; see confocal orthogonal (*YZ*) reconstructions at the bottom.

supplementary material Fig. S6A). In such confluent cells, GFP-mShrm2 was colocalized with the TJ proteins ZO-1 and occludin, whereas only limited colocalization was observed with β-catenin (Fig. 6C).

We then analyzed the kinetics of the junctional targeting of shroom2 in stably transfected MDCK cells producing either GFP-mShrm2 or GFP alone (Fig. 7, and supplementary material Fig. S6C). MDCK cells were pre-treated with trypsin-EDTA to break all the junctions and individualize cells, as described (Nigam et al., 1992; Riesen et al., 2002). Cells were submitted to long-term Ca^{2+} depletion (20 hours in low-Ca^{2+}medium), which resulted in GFP-mShrm2 and ZO-1 localizing in a diffuse pattern or in dot-like cytoplasmic structures (*t*=0 hours in Fig. 7). After restoration of the normal Ca^{2+} concentration, cell-cell contacts were progressively restored. Within 1 hour after addition of Ca^{2+}, MDCK cells producing GFP-mShrm2 or GFP alone displayed the same kinetics of ZO-1 recruitment to the cell-cell junctions (*t*=1 hour in Fig. 7, and supplementary material Fig. S6C). ZO-1 fluorescence intensity displayed a heterogeneous distribution at cell-cell junctions, whereas GFP-mShrm2 was still diffuse in the cytoplasm. Within 2 hours (*t*=2 hours in Fig. 7), GFP-mShrm2 reached the plasma membrane only in cells where ZO-1 was present at cell-cell contacts. Moreover, there was a strong correlation between the GFP-mShrm2 and ZO-1 fluorescent signal intensities at cell-cell junctions (Fig. 7, *t*=2 hours). Within 4, 7 and 24 hours in the presence of Ca^{2+}, ZO-1 and GFP-mShrm2 were homogeneously distributed along the cell-cell contacts, and were especially abundant at tricellular junctions (*t*=7 hours in Fig. 7, and data not shown).

Since the experiments in MDCK cells showed that ZO-1 recruitment at the TJ precedes that of shroom2, we asked whether ZO-1 is sufficient to target shroom2 to the TJ. GFP-mShrm2 was expressed in stably transfected L fibroblasts producing human E-cadherin. These cells (LE cells) form E-cadherin-mediated AJ that contain ZO-1 but lack TJ (Itoh et al., 1993). In non-confluent LE cell cultures, GFP-mShrm2 was found in the cytoplasm, associated with F-actin-rich structures (Fig. 8A), reminiscent of the labeling in non-confluent MDCK cells (Fig. 6A). At cell confluence, GFP-mShrm2 became more diffuse in the cytoplasm, and could not be detected at the cell-cell junctions (Fig. 8B-D). This result indicates that ZO-1 is not sufficient to target shroom2 to cell-cell contacts.

Shroom2 directly interacts with ZO-1

Transfection experiments showed that the PDZ and SPR domains (PSP) of shroom2 are sufficient to target the protein to the cell-cell contacts (supplementary material Fig. S2). To identify putative shroom2-binding partners at the TJ, we thus used a shroom2 fragment that contained the PDZ and SPR domains as the bait (mShrm2PSP; aa 1-356) to screen the inner ear cDNA library in the yeast two-hybrid system (Fig. 9A). We identified two independent clones encoding a ZO-1 fragment

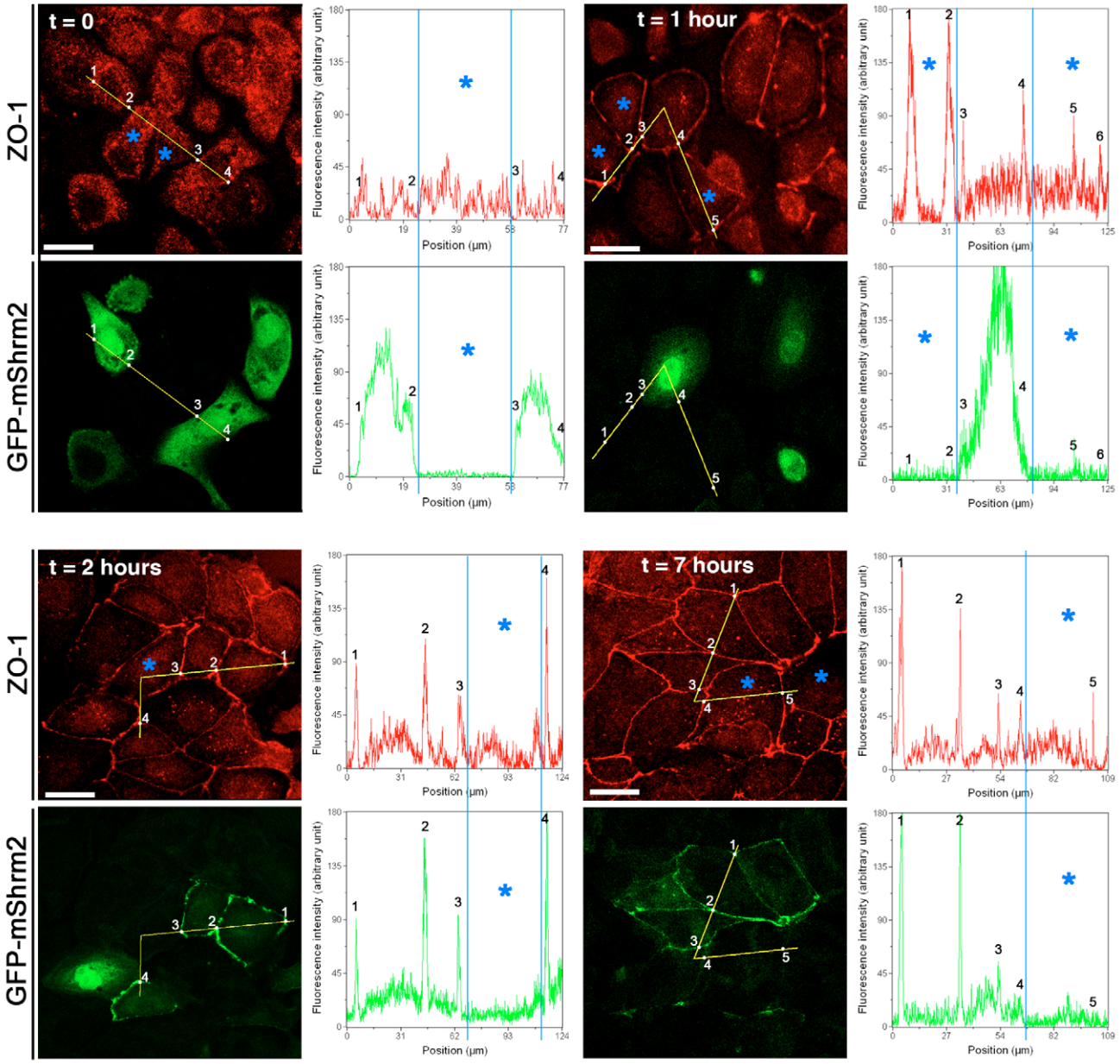

Fig. 7. Shroom2 recruitment at the forming TJs after calcium switch in MDCK cells. The lines were used to calculate the fluorescence intensity in line scan. In micrographs, dots with numbers indicate fluorescence intensity at cell edges. Blue asterisks indicate nontransfected cells that do not express GFP-mShrm2. In the fluorescence intensity profiles, vertical blue lines delineate the emplacement of these cells that were used as an internal control for fluorescence quantification. After 20 hours of incubation in low-Ca^{2+} medium (t=0), cells were fixed and analyzed 1 hour (t=1 hour), 2 hours (t=2 hours) and 7 hours (t=7 hours) after Ca^{2+} repletion. At t=0, the fluorescence intensity profiles of transfected cells indicate that both ZO-1 (red) and GFP-mShrm2 (green) are distributed throughout the cytoplasm. At t=1 hour, ZO-1 is recruited at cell-cell junctions in a discontinuous pattern, whereas GFP-mShrm2 is not yet present at the junctions. At t=2 hours, GFP-mShrm2 is mainly detected at cell-cell junctions and the intensity of the labeling at the junctions correlates with that of ZO-1. At t=7 hours, ZO-1 and GFP-mShrm2 display continuous fluorescence patterns along the junctions, and both protein labelings are more intense at tricellular junctions. Bars, 20 µm.

(aa 444-1015) that contains part of the third PDZ domain, SH3 and guanylate kinase (GuK) domains, and the acid rich region (Fig. 9A). The direct interaction between shroom2 and ZO-1 was confirmed by in vitro binding assays. Either the GST-tagged ZO-1 prey or GST alone was incubated with ^{35}S-labeled shroom2 fragments (Fig. 9B). The GST-tagged ZO-1 prey bound to full-length shroom2 and to mShrm2ΔPDZ (aa 214-1487), but not to mShrm2ASD2 (aa 931-1487; used as an internal control) (Fig. 9B) or MyRIP/Slac2c (used as an unrelated control) (not shown). This result indicates that the shroom2-PDZ domain does not mediate the interaction with ZO-1. Using ^{35}S-labeled shroom2 fragments containing both the PDZ domain and SPR region (mShrm2PSP; aa 1-356), the PDZ domain alone (mShrm2PDZ; aa 1-118) or the SPR region alone (mShrm2SPR; aa 119-356) (Fig. 9B), we found that the SPR region is sufficient for the binding of shroom2 to ZO-1.

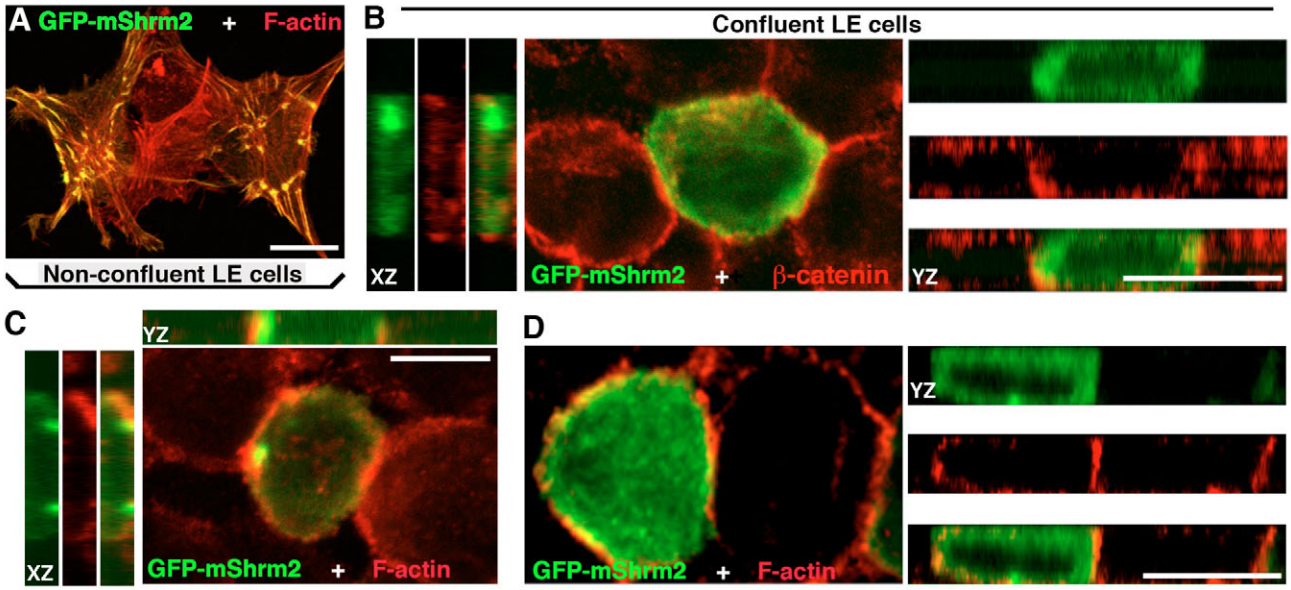

Fig. 8. Shroom2 in mouse L2071 fibroblasts stably transfected with human E-cadherin (LE cells). (A) In non-confluent LE cells that overexpress GFP-mShrm2, the protein is scattered within the cytoplasm or linked to the plasma membrane, associated with F-actin. (B-D) In confluent LE cells, GFP-mShrm2 is not recruited to the cadherin-mediated cell-cell contacts, visualized by (B) β-catenin and (C,D) F-actin. Rather, the GFP-mShrm2 staining is more diffuse, and occasionally forms clusters in the (C, *XZ* plane) basal, or (B, *XZ* and *YZ* planes; C, *YZ* plane) lateral regions of LE cells. Such clusters were not observed in transfected MDCK or Caco-2 cells (see Fig. 6). *XZ* and *YZ* sections show coronal (↑) and orthogonal (→) confocal reconstructions, respectively. Bars, 10 μm.

To determine the site at which ZO-1 binds to shroom2, different ZO-1 fragments fused to GST were produced and incubated with ^{35}S-labeled full-length shroom2 or ^{35}S-labeled SPR domain (mShrm2-SPR) only (Fig. 9C). Shroom2 bound to the SH3/GuK domains of ZO-1 (aa 513-812), whereas a binding was not observed with two ZO-1-truncated fragments containing either the N-terminal PDZ3 and SH3 domains (aa 444-649) or the GuK domain alone (aa 644-812) (Fig. 9C). Shroom2 also failed to bind to ZO-1 fragments encompassing the GuK domain followed by the acid rich region (aa 644-891), or by the entire C-terminal part of the prey (aa 644-1015) (data not shown). We conclude that shroom2, through its SPR domain, binds to ZO-1 within the SH3/GuK domains. In pull-down experiments, overexpressed shroom2 bound to the GST-tagged ZO-1 prey but not to GST alone (supplementary material Fig. S1E). Finally, we were able to coimmunoprecipitate endogenous shroom2 and ZO-1, by using the anti-ZO-1 antibody on auditory organ and brain extracts (Fig. 9D). We conclude that shroom2 and ZO-1 can also interact in vivo.

Discussion

We identified shroom2, a submembranous PDZ-domain-containing protein, as a new binding partner of myosin VIIa, and showed that shroom2 is a TJ protein that also directly interacts with F-actin and ZO-1. Consistent with the results obtained by Dietz et al. (Dietz et al., 2006), we found that shroom2 is present at the AJC in embryonic epithelia. In addition, we show that, in adult mouse epithelia, shroom2 is still present at the AJC and localizes preferentially at the TJs. In transfected epithelial cells expressing shroom2, the protein was not detected in nascent TJs that already contained ZO-1, which indicates that shroom2 is not involved in the early stages of junction formation. Rather, the kinetics of shroom2 recruitment at the forming TJs in the Ca^{2+}-switch experiment suggest that the protein plays a role in TJ stabilization. Indeed, shroom2 contains a PDZ domain and is thus expected to exert a scaffolding function by stabilizing submembranous molecular complexes. Notably, numerous TJ proteins, including the two submembranous proteins ZO-2 and ZO-3, the two groups of integral membrane proteins, JAMs and claudins, possess a typical C-terminal PDZ-binding motif (Schneeberger and Lynch, 2004) and are therefore likely candidates to interact with shroom2. Moreover, because shroom2 can bind to F-actin, it may provide a link between the plasma membrane and the cortical cytoskeleton at the TJ. Our results further suggest that the shroom2 MBR subdomain stabilizes actin filaments because it was able to protect F-actin from cytochalasin-D-induced disruption in transfected MDCK cells. Finally, the abundance of shroom2 at TJs in mature epithelia, which are very tight (e.g. marginal cell layer of the cochlear stria vascularis) (Jahnke, 1975) or are continuously submitted to shearing forces (e.g. reticular lamina of the organ of Corti) (Nowotny and Gummer, 2006), further supports the idea that shroom2 is involved in the strengthening of the TJs.

There is increasing evidence that the TJ, on its cytoplasmic side, acts as a platform where the trafficking of proteins to the apical versus basolateral zone is controlled (Kohler and Zahraoui, 2005). In the AJC region, structural proteins (actin, microtubules, spectrin) and regulatory proteins (actin-binding proteins, GTPases, kinases) are juxtaposed with transmembrane proteins (Matter and Balda, 2003; Schneeberger and Lynch, 2004; Kohler and Zahraoui, 2005). The clustering of Rabs, their effectors and the Sec6-Sec8 complex close to the TJ has been proposed to provide the machinery required for docking and fusion of transport vesicles

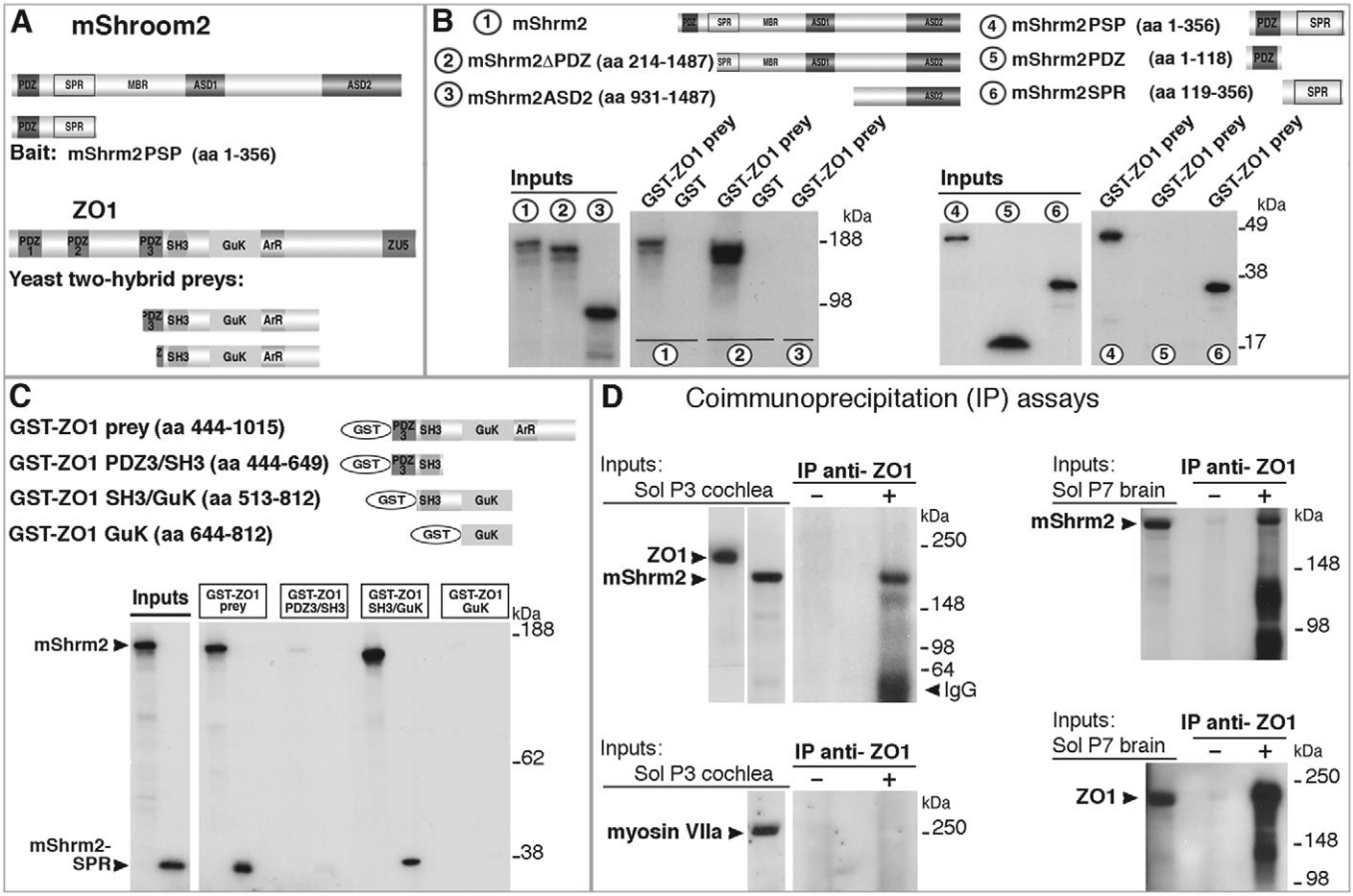

Fig. 9. Shroom2 binds to ZO-1 in vitro and in vivo. (A) Domain structure of the shroom2 yeast two-hybrid bait (mShrm2PSP) and of the two ZO-1 preys isolated. (B) Several ^{35}S-labeled shroom2 fragments (labeled 1 to 6) were incubated with the GST-tagged ZO-1 prey (GST- ZO1 prey) or GST alone. mShrm2, mShrm2ΔPDZ, mShrm2PSP and mShrm2SPR bind to the GST- ZO1 prey, but not to GST. By contrast, mShrm2ASD2 and mShrm2PDZ do not bind to the GST-ZO1 prey. (C) Characterization of the shroom2-interaction domain of ZO-1. ^{35}S-labeled shroom2 and ^{35}S-labeled shroom2-SPR only bind to the original GST-ZO1 prey and to the GST-ZO1 SH3/GuK fragment. (D) Protein extracts from the mouse auditory organ (left panels) or brain (right panels) were used for the immunoprecipitation assays. The endogenous shroom2 protein is immunoprecipitated in the presence of the anti-ZO-1 antibody, but not with protein G alone. Under the conditions we used, ZO-1 immunoprecipitates do not contain myosin VIIa (bottom panels).

(see Kohler and Zahraoui, 2005). Shroom2 displays a wider tissue distribution compared with that of myosin VIIa, but both proteins are present in a variety of epithelial cells, including hair cells, retinal pigment epithelium cells, choroid plexus cells, enterocytes and kidney tubular cells (Sahly et al., 1997; Wolfrum et al., 1998). In these cells, myosin VIIa can be detected throughout the cell body, and electron microscopy analyses have shown that this myosin is especially abundant in ciliary and microvillar structures (Sahly et al., 1997; Wolfrum et al., 1998). In hair cells, myosin VIIa – like shroom2 – is especially abundant in the vesicle-rich region at the immediate vicinity of the AJC (Hasson et al., 1997). How then, does myosin VIIa act in conjunction with shroom2? It has been shown in vitro that dimerized myosin VIIa can move processively on actin filaments, and myosin VIIa requires high ATP concentrations for its motile activity (Inoue and Ikebe, 2003; Yang et al., 2006). By contrast, ADP increases the F-actin-binding affinity of myosin VIIa to actin filaments, suggesting that in subcellular compartments with a high ADP concentration, myosin VIIa is exerting a tension force (Inoue and Ikebe, 2003) rather than having a transport function. Collectively, its kinetic parameters would allow myosin VIIa to exert and hold tension on actin filaments and, when dimerized, to function as a processive cargo transporter. Therefore, depending on the ATP context in situ, myosin VIIa, in conjunction with shroom2, could be involved in the targeting of a certain set of proteins and/or vesicles at the TJ.

Fairbank et al. have reported that a loss of shroom2 activity results in defects in both the biogenesis and the apical localization of retinal melanosomes in *Xenopus* (Fairbank et al., 2006). It is worthy of note that also in myosin-VIIa-defective mice, melanosomes do not enter the apical processes in retinal pigment epithelium cells (Liu et al., 1998). Myosin VIIa and shroom2 codistribute at the level of the TJ zone, whereas myosin VIIa and its binding partner MyRIP are especially abundant in the apical microvilli (El-Amraoui et al., 2002). Therefore, in the retinal pigment epithelium cells, the putative interaction between shroom2 and myosin VIIa could be essential to transfer melanosomes from microtubules to the apical actin cytoskeleton in the TJ zone. Once in the microvilli,

a tripartite complex of myosin VIIa, MyRIP/Slac2c and Rab27a would mediate the recruitment and movement of melanosomes along the peripheral actin filaments (El-Amraoui et al., 2002; Fukuda and Kuroda, 2002). This scenario is in agreement with the recent results showing that, in addition to their link to F-actin, proteins of the shroom family regulate γ-tubulin distribution and may thus coordinate the assembly of both microtubule and actin cytoskeletons (Fairbank et al., 2006; Lee et al., 2007).

Among the shroom family members, shroom2 displays the same modular organization as shroom3a, namely a N-terminal PDZ domain and two C-terminal ASD domains (see supplementary material Fig. S7A). In primary neural tube cells from mouse embryos, shroom3a is located at the AJs (Hildebrand and Soriano, 1999). Shroom3 regulates the formation of a contractile actomyosin network associated with the AJC, and it has been proposed that shroom3 regulates the distribution of myosin II at the AJC (Hildebrand, 2005). Therefore, we propose that through interactions between shroom2 and myosin VIIa, and shroom3a and myosin II, similar interaction networks between the plasma membrane and subcortical actin cytoskeleton takes place at the TJ and AJ, respectively (see supplementary material Fig. S7B).

Materials and Methods

Yeast two-hybrid screenings and expression constructs

Yeast two-hybrid screenings were performed as described previously (Rain et al., 2001) using different baits, namely the C-terminal SH3/MyTH4/FERM fragment of myosin VIIa (aa 1605-2215), and the N-terminal PDZ and SPR domains of shroom2 (mShrm2PSP, aa 1-356).

The full-length mouse cDNA encoding shroom2 (GenBank accession number EF071946) was reconstituted by using race-PCR on a mouse inner ear cDNA library and sequence comparison with ESTs. PCR-amplified fragments of myosin VIIa, shroom2 and ZO-1 cDNA were checked prior to transfer to the appropriate expression vector. Inserts were subcloned into pEGFP (Clontech), pCDNA-DEST-47/53 (Invitrogen), pCMV-tag3B (Myc tag, Stratagene) and pcDNA3 (No tag or V5/His, Invitrogen) for in vitro translation and transfection experiments, and into pGEX-4T1 (GST tag, Amersham) and pXa3 (biotin tag, Promega) for protein production.

The following fragments were subcloned into the appropriate vectors. For myosin VIIa: myosin VIIa tail (aa 847-2215), SH3/MyTH4/FERM fragment (aa 1612-2215), MyTH4/FERM fragment (aa 1752-2215), SH3/MyTH4 fragment (aa 1605-1907), MyTH4 domain (aa 1752-1890) and FERM domain (aa 1896-2215). For shroom2: PDZ domain (aa 1-118), SPR domain (aa 119-356), PSP fragment (aa 1-356), the myosin VIIa-binding region (MBR, aa 350-721), MBR-ASD1 fragment (aa 293-810) and ASD2-containing fragment (aa 931-1487). The truncated mShrm2MBR fragment (mShrm2MBRΔC) was produced by introducing a stop codon at aa position 563, using the quick-change mutagenesis system, according to the supplier's instructions (Stratagene). For ZO-1: SH3/GuK fragment (aa 513-812), part of the PDZ3 domain and SH3 domain (aa 444-649); GuK domain (aa 644-812); GuK/acid-rich region fragment (aa 644-891); GuK/acid-rich region/C-terminal part of the prey (aa 644-1015).

Binding experiments

The in vitro binding assays were performed using glutathione-Sepharose (Amersham) and/or Tetra-link avidin resins (Promega) as described (Kussel-Andermann et al., 2000). Radiolabeled proteins were translated in vitro with the T7/T3-coupled transcription-translation system (Promega) according to the manufacturer's instructions. To test the interaction between shroom2 and myosin VIIa, a bacterial lysate containing the GST-mShrm2MBR fusion peptide was incubated with pre-equilibrated glutathione-Sepharose beads for 90 minutes at 4°C. The beads were washed three times with binding buffer (5% glycerol, 5 mM $MgCl_2$ and 0.1% Triton X-100 in PBS) supplemented with a protease inhibitor cocktail (Roche), and then incubated with the in vitro translated ^{35}S-labeled myosin VIIa fragments for 3 hours at 4°C on a rotating wheel. Beads were then washed four times with binding buffer supplemented with 150 mM NaCl. Bound proteins were resuspended in 30 μl 2× concentrated SDS sample buffer, and analyzed on a 4-12% SDS-PAGE.

Co-immunoprecipitation of Myc-tagged shroom2 and either the myosin VIIa tail or full-length myosin VIIa was done using monoclonal anti-Myc antibodies (Santa Cruz). HEK-293 cell extracts were prepared using 500 μl of lysis buffer (0.1% Triton X-100, and 0.1% sodium deoxycholate, 0.5 mM DTT, protease inhibitor cocktail in PBS pH 7.4). The anti-Myc-preincubated resin was incubated with the soluble fraction for 2 hours at 4°C, and washed four times in 0.1% Triton-X100 with protease inhibitor cocktail in PBS. Samples were analyzed as mentioned above.

Co-immunoprecipitation of ZO-1 and shroom2 in vivo. Cochleas from mice at postnatal day 3 (P3) or P4, or brains from mice at P7 were homogenized in 500 μl lysis buffer (20 mM Tris pH 7.5, 200 mM NaCl, 1 mM $MgCl_2$, 0.2% Triton X-100, 0.01% SDS, 1% glycerol, and protease inhibitor cocktail). The soluble fraction was incubated for 2 hours with 40 μl protein G-agarose preincubated either with 3 μg of purified anti-ZO-1 polyclonal antibody (Zymed) or without antibody. After three washes in PBS supplemented with 25 mM NaCl and 0.1% Triton X-100, bound complexes were resuspended in 20 μl SDS sample buffer, and analyzed on a 3-8% Tris-glycine SDS-PAGE.

Actin binding assays

A solution of 50 μM G-actin (Molecular Probes) was polymerized by incubation for 30 minutes at 37°C in a high-salt buffer containing 50 mM KCl and 2 mM $MgCl_2$. Co-sedimentation assays were done by incubating 2 μg of either GST-mShrm2MBR or GST, with 20 μl of a 16.5 μM F-actin solution for 30 minutes, followed by ultracentrifugation (100,000 ***g***, 1 hour). The same amount of supernatant and pellet fractions were subjected to SDS-PAGE and analyzed with Coomassie Blue staining.

Antibodies and immunofluorescence analysis

A polyclonal antibody was produced against a mixture of two peptides derived from the murine shroom2 protein: mShrm2P1 (MEGAEPRARPERLAE, aa 1-15) and mShrm2P2 (GSFPSTYKEHLKEAQ, aa 695-709). Antibodies from two rabbits (R1 and R2) were used. The specificity of the immunopurified antibodies was assayed by immunocytofluorescence and immunoblot analysis. Substitution of the preimmune serum for the purified antibody against shroom2 and preadsorption of the antibodies with the corresponding antigens were used as negative controls.

The following monoclonal antibodies were used: anti-ZO-1 (Zymed), anti-occludin (Zymed), anti-E-cadherin (Transduction laboratories), anti-β-catenin (Transduction laboratories), anti-GST (Amersham). F-actin was visualized using TRITC-phalloidin (Sigma).

Immunofluorescence analyses were carried out on fixed cells (grown on glass coverslips or on transwell filters) and cryostat sections of tissues or whole-mount preparations of the organ of Corti of RJ Swiss mice (Janvier, France) as described previously (Kussel-Andermann et al., 2000). Cells, tissue sections and whole-mount preparations were analyzed with a laser scanning confocal microscope (LSM-540, Zeiss).

Cells, transfection and Ca^{2+}-switch assays

HeLa, Caco-2, MDCK, LLCPK, CHO, L and LE cells were grown in DMEM supplemented with 10% FCS, containing penicillin and streptomycin. Transient transfections were performed using Effectene (Qiagen) for HeLa and CHO cells and Lipofectamine Plus (Invitrogen) for the other cell lines, according to the manufacturer's instructions. Stable MDCK cell lines expressing GFP-mShrm2 and GFP alone were obtained by Jet-PEI transfection agent (Polyplus-transfection). Cells were treated with 0.8 mg/ml G418 (PAA) for 10 days to select stable transfectants. Cells were then sorted by FACS using MoFlo setup of the Pasteur Institute cytometry platform. We selected small subpopulations for a weak intensity of fluorescence to avoid very high levels of transgene expression. Stable cell lines were maintained under selection in 0.2 mg/ml G418. For the Ca^{2+}-switch experiments, 1.3×10^5 MDCK cells/cm^2 were grown overnight (20 hours) in low-Ca^{2+} medium i.e. Ca^{2+}-free D-MEM supplemented with 5% dialyzed FCS (Invitrogen), according to the protocol by Gumbiner (Gumbiner et al., 1988). Cells were then incubated in D-MEM containing physiological concentrations of Ca^{2+} for 0, 1, 2, 4, 7 and 24 hours, fixed in 4% PFA and analyzed by immunofluorescence. Fluorescence intensity profile analysis was performed using the linescan function of MetaMorph (version 7.0, Universal Imaging Corp., Downingtown, PA) as described (Sousa et al., 2005). The profile of fluorescence intensity was measured along the line in two channels.

We thank S. Blanchard, S. Nouaille, A. Louise, H. Kiefer, M. C. Wagner and V. Michel for technical assistance, and J.-P. Hardelin for critical reading of the manuscript. This work was supported by grants from Fondation Raymonde et Guy Strittmatter, the European Commission FP6 Integrated Project EuroHear LSHG-CT-2004-512063, ANR-05-MRAR-015-01, Ernst-Jung Stiftung für Medizin Preis, and A & M Suchert-Retina Kontra Blindheit. The confocal microscope was purchased with a donation from Marcel and Liliane Pollack. I.Z. and R.E. received a fellowship from Fondation pour la Recherche Médicale (France).

References

Bershadsky, A. (2004). Magic touch: how does cell-cell adhesion trigger actin assembly? *Trends Cell Biol.* **14**, 589-593.

Boeda, B., El-Amraoui, A., Bahloul, A., Goodyear, R., Daviet, L., Blanchard, S., Perfettini, I., Fath, K. R., Shorte, S., Reiners, J. et al. (2002). Myosin VIIa, harmonin and cadherin 23, three Usher I gene products that cooperate to shape the sensory hair cell bundle. *EMBO J.* **21**, 6689-6699.

Cordenonsi, M., D'Atri, F., Hammar, E., Parry, D. A., Kendrick-Jones, J., Shore, D. and Citi, S. (1999). Cingulin contains globular and coiled-coil domains and interacts with ZO-1, ZO-2, ZO-3, and myosin. *J. Cell Biol.* **147**, 1569-1582.

Dermietzel, R. and Kroczek, H. (1980). Interlamellar tight junctions of central myelin. I. Developmental mechanisms during myelogenesis. *Cell Tissue Res.* **213**, 81–94.

Dietz, M. L., Bernaciak, T. M., Vendetti, F., Kielec, J. C. and Hildebrand, J. D. (2006). Differential actin-dependent localization modulates the evolutionarily conserved activity of Shroom family proteins. *J. Biol. Chem.* **281**, 20542-20554.

El-Amraoui, A. and Petit, C. (2005). Usher I syndrome: unravelling the mechanisms that underlie the cohesion of the growing hair bundle in inner ear sensory cells. *J. Cell Sci.* **118**, 4593-4603.

El-Amraoui, A., Schonn, J. S., Kussel-Andermann, P., Blanchard, S., Desnos, C., Henry, J. P., Wolfrum, U., Darchen, F. and Petit, C. (2002). MyRIP, a novel Rab effector, enables myosin VIIa recruitment to retinal melanosomes. *EMBO Rep.* **3**, 463-470.

Fairbank, P. D., Lee, C., Ellis, A., Hildebrand, J. D., Gross, J. M. and Wallingford, J. B. (2006). Shroom2 (APXL) regulates melanosome biogenesis and localization in the retinal pigment epithelium. *Development* **133**, 4109-4118.

Fanning, A. S. (2001). Organization and regulation of the tight junctions by the actin-myosin cytoskeleton. In *Tight Junctions* (ed. J. M. Anderson and M. Cereijido), pp. 265-284. Boca Raton, FL: CRC Press.

Fukuda, M. and Kuroda, T. S. (2002). Slac2-c (synaptotagmin-like protein homologue lacking C2 domains-c), a novel linker protein that interacts with Rab27, myosin Va/VIIa, and actin. *J. Biol. Chem.* **277**, 43096-43103.

Gumbiner, B., Stevenson, B. and Grimaldi, A. (1988). The role of the cell adhesion molecule uvomorulin in the formation and maintenance of the epithelial junctional complex. *J. Cell Biol.* **107**, 1575-1587.

Hagens, O., Ballabio, A., Kalscheuer, V., Kraehenbuhl, J. P., Schiaffino, M. V., Smith, P., Staub, O., Hildebrand, J. and Wallingford, J. B. (2006). A new standard nomenclature for proteins related to Apx and Shroom. *BMC Cell Biol.* **7**, 18.

Hasson, T., Gillespie, P. G., Garcia, J. A., MacDonald, R. B., Zhao, Y., Yee, A. G., Mooseker, M. S. and Corey, D. P. (1997). Unconventional myosins in inner-ear sensory epithelia. *J. Cell Biol.* **137**, 1287-1307.

Hildebrand, J. D. (2005). Shroom regulates epithelial cell shape via the apical positioning of an actomyosin network. *J. Cell Sci.* **118**, 5191-5203.

Hildebrand, J. D. and Soriano, P. (1999). Shroom, a PDZ domain-containing actin-binding protein, is required for neural tube morphogenesis in mice. *Cell* **99**, 485-497.

Inoue, A. and Ikebe, M. (2003). Characterization of the motor activity of mammalian myosin VIIA. *J. Biol. Chem.* **278**, 5478-5487.

Itoh, M., Nagafuchi, A., Yonemura, S., Kitani-Yasuda, T. and Tsukita, S. (1993). The 220-kD protein colocalizing with cadherins in non-epithelial cells is identical to ZO-1, a tight junction-associated protein in epithelial cells: cDNA cloning and immunoelectron microscopy. *J. Cell Biol.* **121**, 491-502.

Ivanov, A. I., Hunt, D., Utech, M., Nusrat, A. and Parkos, C. A. (2005a). Differential roles for actin polymerization and a myosin II motor in assembly of the epithelial apical junctional complex. *Mol. Biol. Cell* **16**, 2636-2650.

Ivanov, A. I., Nusrat, A. and Parkos, C. A. (2005b). Endocytosis of the apical junctional complex: mechanisms and possible roles in regulation of epithelial barriers. *BioEssays* **27**, 356-365.

Jahnke, K. (1975). The fine structure of freeze-fractured intercellular junctions in the guinea pig inner ear. *Acta Otolaryngol. Suppl.* **336**, 1-40.

Kohler, K. and Zahraoui, A. (2005). Tight junction: a co-ordinator of cell signalling and membrane trafficking. *Biol. Cell* **97**, 659-665.

Krendel, M. and Mooseker, M. S. (2005). Myosins: tails (and heads) of functional diversity. *Physiology Bethesda* **20**, 239-251.

Kussel-Andermann, P., El-Amraoui, A., Safieddine, S., Nouaille, S., Perfettini, I., Lecuit, M., Cossart, P., Wolfrum, U. and Petit, C. (2000). Vezatin, a novel transmembrane protein, bridges myosin VIIA to the cadherin-catenins complex. *EMBO J.* **19**, 6020-6029.

Lee, C., Scherr, H. M. and Wallingford, J. B. (2007). Shroom family proteins regulate {gamma}-tubulin distribution and microtubule architecture during epithelial cell shape change. *Development* **134**, 1431-1441.

Liu, X., Ondek, B. and Williams, D. S. (1998). Mutant myosin VIIa causes defective melanosome distribution in the RPE of shaker-1 mice. *Nat. Genet.* **19**, 117-118.

Liu, X., Udovichenko, I. P., Brown, S. D., Steel, K. P. and Williams, D. S. (1999). Myosin VIIa participates in opsin transport through the photoreceptor cilium. *J. Neurosci.* **19**, 6267-6274.

Madara, J. L. (1998). Regulation of the movement of solutes across tight junctions. *Annu. Rev. Physiol.* **60**, 143-159.

Matter, K. and Balda, M. S. (2003). Signalling to and from tight junctions. *Nat. Rev. Mol. Cell Biol.* **4**, 225-236.

Miyoshi, J. and Takai, Y. (2005). Molecular perspective on tight-junction assembly and epithelial polarity. *Adv. Drug Deliv. Rev.* **57**, 815-855.

Mooseker, M. S. (1985). Organization, chemistry, and assembly of the cytoskeletal apparatus of the intestinal brush border. *Annu. Rev. Cell Biol.* **1**, 209-241.

Nigam, S. K., Rodriguez-Boulan, E. and Silver, R. B. (1992). Changes in intracellular calcium during the development of epithelial polarity and junctions. *Proc. Natl. Acad. Sci. USA* **89**, 6162-6166.

Nowotny, M. and Gummer, A. W. (2006). Nanomechanics of the subtectorial space caused by electromechanics of cochlear outer hair cells. *Proc. Natl. Acad. Sci. USA* **103**, 2120-2125.

Perez-Moreno, M., Jamora, C. and Fuchs, E. (2003). Sticky business: orchestrating cellular signals at adherens junctions. *Cell* **112**, 535-548.

Rain, J. C., Selig, L., De Reuse, H., Battaglia, V., Reverdy, C., Simon, S., Lenzen, G., Petel, F., Wojcik, J., Schachter, V. et al. (2001). The protein-protein interaction map of Helicobacter pylori. *Nature* **409**, 211-215.

Riesen, F. K., Rothen-Rutishauser, B. and Wunderli-Allenspach, H. (2002). A ZO1-GFP fusion protein to study the dynamics of tight junctions in living cells. *Histochem. Cell Biol.* **117**, 307-315.

Sahly, I., El-Amraoui, A., Abitbol, M., Petit, C. and Dufier, J. L. (1997). Expression of myosin VIIA during mouse embryogenesis. *Anat. Embryol.* **196**, 159-170.

Schneeberger, E. E. and Lynch, R. D. (2004). The tight junction: a multifunctional complex. *Am. J. Physiol. Cell Physiol.* **286**, C1213-C1228.

Self, T., Mahony, M., Fleming, J., Walsh, J., Brown, S. D. and Steel, K. P. (1998). Shaker-1 mutations reveal roles for myosin VIIA in both development and function of cochlear hair cells. *Development* **125**, 557-566.

Shewan, A. M., Maddugoda, M., Kraemer, A., Stehbens, S. J., Verma, S., Kovacs, E. M. and Yap, A. S. (2005). Myosin 2 is a key rho kinase target necessary for the local concentration of e-cadherin at cell-cell contacts. *Mol. Biol. Cell* **16**, 4531-4542.

Sousa, S., Cabanes, D., Archambaud, C., Colland, F., Lemichez, E., Popoff, M., Boisson-Dupuis, S., Gouin, E., Lecuit, M., Legrain, P. et al. (2005). ARHGAP10 is necessary for alpha-catenin recruitment at adherens junctions and for Listeria invasion. *Nat. Cell Biol.* **7**, 954-960.

Staub, O., Verrey, F., Kleyman, T. R., Benos, D. J., Rossier, B. C. and Kraehenbuhl, J. P. (1992). Primary structure of an apical protein from *Xenopus laevis* that participates in amiloride-sensitive sodium channel activity. *J. Cell Biol.* **119**, 1497-1506.

Turner, J. R. (2000). 'Putting the squeeze' on the tight junction: understanding cytoskeletal regulation. *Semin. Cell Dev. Biol.* **11**, 301-308.

Vasioukhin, V., Bauer, C., Yin, M. and Fuchs, E. (2000). Directed actin polymerization is the driving force for epithelial cell-cell adhesion. *Cell* **100**, 209-219.

Velichkova, M., Guttman, J., Warren, C., Eng, L., Kline, K., Vogl, A. W. and Hasson, T. (2002). A human homologue of Drosophila kelch associates with myosin-VIIa in specialized adhesion junctions. *Cell Motil. Cytoskeleton* **51**, 147-164.

Verma, S., Shewan, A. M., Scott, J. A., Helwani, F. M., den Elzen, N. R., Miki, H., Takenawa, T. and Yap, A. S. (2004). Arp2/3 activity is necessary for efficient formation of E-cadherin adhesive contacts. *J. Biol. Chem.* **279**, 34062-34070.

Weil, D., Blanchard, S., Kaplan, J., Guilford, P., Gibson, F., Walsh, J., Mburu, P., Varela, A., Levilliers, J., Weston, M. D. et al. (1995). Defective myosin VIIA gene responsible for Usher syndrome type 1B. *Nature* **374**, 60-61.

Wolfrum, U., Liu, X., Schmitt, A., Udovichenko, I. P. and Williams, D. S. (1998). Myosin VIIa as a common component of cilia and microvilli. *Cell Motil. Cytoskeleton* **40**, 261-271.

Yang, Y., Kovacs, M., Sakamoto, T., Zhang, F., Kiehart, D. P. and Sellers, J. R. (2006). Dimerized Drosophila myosin VIIa: a processive motor. *Proc. Natl. Acad. Sci. USA* **103**, 5746-57451.

Zuckerman, J. B., Chen, X., Jacobs, J. D., Hu, B., Kleyman, T. R. and Smith, P. R. (1999). Association of the epithelial sodium channel with Apx and alpha-spectrin in A6 renal epithelial cells. *J. Biol. Chem.* **274**, 23286-23295.